Numerical modeling of light propagation in biological tissues: time-resolved 3D simulations based on light diffusion model and FDTD solution of Maxwell's equations

N. Ortega-Quijano[a], O. G. Romanov[b], F. Fanjul-Vélez[a], I. Salas-García[a], A. L. Tolstik[b], J. L. Arce-Diego[*a]

[a] Applied Optical Techniques Group, TEISA Department, University of Cantabria, Av. de los Castros s/n, 39005 Santander, Spain

[b] Laser Physics and Spectroscopy Department, Belarusian State University, Nezalezhnasty Ave. 4, 220030 Minsk, Belarus

ABSTRACT

In this work, optical propagation through turbid media is analyzed by FDTD simulation. In particular, the method is applied to biological tissues. Continuous light propagation in turbid media has been widely studied, but pulsed light propagation has received less interest due to its complexity. Therefore, in this work we focus on pulsed light. FDTD method is applied to several media with optical parameters in the typical range of those observed in biological tissues. We perform an analysis of the variations of pulsed light propagation as a function of the scatterers characteristics (namely size, concentration, and optical contrast). The results are compared with those obtained by the use of the diffusion approximation. The potential of the FDTD method over the diffusion model is given by its high accuracy, its capacity to perform time-resolved simulations, and the fact that it carries all the information about the phase and coherence of the wavefront. The results of this work can be applied to a wide range of areas of interest like the time-resolved study of ultrashort light pulses propagation, the optimization of optical penetration depth, the coherence properties of pulsed light, and the effect of modified wavefronts in light propagation.

Keywords: biological tissues, scattering, FDTD, diffusion approximation, pulsed light

1. INTRODUCTION

There exist several models for light beam propagation, from which the most widely used ones are the slowly varying envelope approximation of the wave equation [1], the Radiation Transport Theory (RTT) [2], the Monte-Carlo method (MC) [3], and the finite-difference time-domain method (FDTD) for direct solution of Maxwell's equations [4].

If the initial intensity of light beam is insufficient to activate nonlinear effects and the propagation distance is less than the diffractive length, then the slowly varying envelope approximation is valid, and propagation of the light beam can be considered simply from Beer-Lambert law. The results obtained by means of this approach present low accuracy, specially when dealing with complex multilayered or strongly anisotropic scattering tissues. Radiation Transport Theory is usually applied when scattering is dominating over absorption, and it is based on a light-diffusion equation for calculating the fluence rate. The relationship with the Beer-Lambert law can be established with the use of the so-called effective attenuation coefficient. In the Monte Carlo method light is treated as a sequence of photons. The number of photons is related to the accuracy of the solution obtained. After launching a photon, its trajectory is calculated. This trajectory is affected by scattering and absorption. Monte Carlo method provides a steady-state solution for light propagation in turbid media, and as a consequence the effects of pulsed propagation are neglected.

The finite-diference time-domain method (FDTD) is a very powerful approach for solving Maxwell's equations, and is the focus of this work. The potential of this method is given by its high accuracy and by the fact that it carries all the information about the phase and coherence of the wavefront. Due to its accuracy, the FDTD method is widely used in simulating light propagation in optical waveguides like optical fibers or photonic crystals, for example. This method was

[*] arcedj@unican.es; phone +34 942 20 15 45; fax +34 942 20 18 73; www.teisa.unican.es/toa

Diffuse Optical Imaging III, edited by Andreas H. Hielscher, Paola Taroni, Proc. of SPIE-OSA Biomedical Optics, SPIE Vol. 8088, 80881R · © 2011 SPIE-OSA · CCC code: 1605-7422/11/$18 · doi: 10.1117/12.889826

applied to the study of light propagation in biological tissues. Continuous light propagation in turbid media has been widely studied, but pulsed light propagation has received less interest due to its complexity. Therefore, in this work we analyse propagation of pulsed light. The parameters of the medium used in the simulations were chosen according to the typical characteristics of biological tissues [5]. We perform an analysis of the variations of the pulses light propagation as a function of the scatterers characteristics (namely size, concentration, and optical contrast). The results are compared with those obtained by the use of the diffusion approximation. The potential of the FDTD method over the diffusion model is given by its high accuracy, its capacity to perform time-resolved simulations, and the fact that it carries all the information about the phase and coherence of the wavefront [6,7].

The manuscript is organized as follows. First of all, the light propagation models employed are presented in Section 2. Section 2.1 is devoted to light diffusion equation, and in section 2.2 the basic equations of the FDTD algorithm are shown, both for TE and TM mode. The main results of the simulations are included in Section 3, as long as the discussion. Finally, in Section 4 we summarize the conclusions of this work.

2. MODELS OF LIGHT PROPAGATION IN BIOLOGICAL TISSSUES

In this section we introduce the light propagation models that will be used through the manuscript. Section 2.1 describes light diffusion equation, and section 2.2 explains the FDTD approach.

2.1 Light diffusion equation

Radiation Transport Theory is a widely used method for modeling light propagation in terms of the specific intensity of optical radiation. When scattering presents a dominant effect over absorption, the diffusion approximation can be applied for obtaining the analytical solution of the Radiation Transport Equation. In the diffusion model, tissues are characterized, from the point of view of optical propagation, by the following parameters: refractive index n; reduced scattering coefficient $\mu_s' = (1-g)\mu_s$, where g is the anisotropy of scattering and μ_s is the scattering coefficient; and absorption coefficient μ_a. In the scattering-dominant limit, the medium is characterized by the diffusion constant $D = 1/3(\mu_a + \mu_s')$. The diffusion model describes light propagation by a diffusion equation, which can be expressed in the following way [2]:

$$\frac{1}{v}\frac{\partial\phi(\vec{r},t)}{\partial t} + \mu_a\phi(\vec{r},t) - \nabla\left[D\nabla\phi(\vec{r},t)\right] = S(\vec{r},t). \tag{1}$$

In this equation, $\phi(\vec{r},t)$ represents the irradiance in the tissue, and $S(\vec{r},t)$ takes into account the optical source power per unit volume. Equation (1) provides a spatial-temporal solution for the optical distribution inside an irradiated tissue. Considering the problem of light pulse propagation in semi-infinite media the boundary conditions for the plane z=0 can be expressed as: $\phi(\vec{r},t) - 2C_R D\frac{\partial\phi(\vec{r},t)}{\partial z} = 0$, where the coefficient C_R takes into account Fresnel reflection on the boundary between tissue and air. The intensity distribution in pulsed Gaussian-like light beam presents this form: $I(x,y,z=0,t) = I_0 \exp\left(-\frac{x^2+y^2}{r_0^2}\right)\frac{t}{t_p}\exp\left(-\frac{t}{t_p}\right)$. A finite difference numerical method can be used to obtain a solution for the fluence rate. After normalization we obtain the following equation:

$$\left(\frac{\partial^2}{\partial\xi^2} + \frac{\partial^2}{\partial\eta^2} + \frac{\partial^2}{\partial\zeta^2}\right)\varphi(\xi,\eta,\zeta,\tau) = a_1\frac{\partial\varphi(\xi,\eta,\zeta,\tau)}{\partial\tau} + a_2\varphi(\xi,\eta,\zeta,\tau), \tag{2}$$

where fluence φ, time τ and spatial (ξ,η,ζ) coordinates are normalized variables through: $\varphi = \phi / I_0$; $\tau = t/t_0$ (t_0 is a characteristic time); $\xi = x/r_0$; $\eta = y/r_0$; $\zeta = z/r_0$; and the dimensionless parameters $a_1 = r_0^2 / Dvt_0$, $a_2 = \mu_a r_0^2 / D$. We apply the 3D generalization of the method developed by Du Fort and Frankel [8, 9] for the numerical approximation of parabolic partial differential equations, which was successfully used in our work previous work [5]. The following finite different approximation of Eq. (2) was used:

$$\varphi_{i,j,k,l+1} = \frac{\gamma}{\theta}\varphi_{i,j,k,l-1} + \frac{1}{\theta}\left(\frac{1}{\omega_\xi}\left(\varphi_{i+1,j,k,l} + \varphi_{i-1,j,k,l}\right) + \frac{1}{\omega_\eta}\left(\varphi_{i,j+1,k,l} + \varphi_{i,j-1,k,l}\right) + \frac{1}{\omega_\zeta}\left(\varphi_{i,j,k+1,l} + \varphi_{i,j,k-1,l}\right)\right), \quad (3)$$

where the coefficients $\theta, \gamma = 1 \pm \frac{2\Delta\tau}{a_1}\left(\frac{1}{\Delta\xi^2} + \frac{1}{\Delta\eta^2} + \frac{1}{\Delta\zeta^2}\right) \pm \frac{2\Delta\tau a_2}{a_1}$. The results of numerical simulations are discussed in Section 3.

2.2 FDTD numerical approach

Among the different methods to study light propagation through random media, finite-difference time-domain technique constitutes a very powerful one, as long as it carries all the information about the phase and coherence of the wavefront. FDTD is a widely used technique that numerically solves Maxwell's equations with a high accuracy, entailing a considerable computing time. We start from Maxwell's equations for an optical medium [4]:

$$-\mu_0 \frac{\partial \vec{H}}{\partial t} = \nabla \times \vec{E}\,, \quad (4)$$

$$\varepsilon_0 \varepsilon(x,y,z) \frac{\partial \vec{E}}{\partial t} = \nabla \times \vec{H}\,. \quad (5)$$

These equations can be decomposed into the three coordinate components to obtain a set of six differential equations:

$$\frac{\partial H_x}{\partial t} = -\frac{1}{\mu_0}\left[\frac{\partial E_z}{\partial y} - \frac{\partial E_y}{\partial z}\right], \quad (6)$$

$$\frac{\partial H_y}{\partial t} = -\frac{1}{\mu_0}\left[\frac{\partial E_x}{\partial z} - \frac{\partial E_z}{\partial x}\right], \quad (7)$$

$$\frac{\partial H_z}{\partial t} = -\frac{1}{\mu_0}\left[\frac{\partial E_y}{\partial x} - \frac{\partial E_x}{\partial y}\right], \quad (8)$$

$$\frac{\partial E_x}{\partial t} = \frac{1}{\varepsilon_0 \varepsilon(x,y,z)}\left[\frac{\partial H_z}{\partial y} - \frac{\partial H_y}{\partial z}\right], \quad (9)$$

$$\frac{\partial E_y}{\partial t} = \frac{1}{\varepsilon_0 \varepsilon(x,y,z)}\left[\frac{\partial H_x}{\partial z} - \frac{\partial H_z}{\partial x}\right], \quad (10)$$

$$\frac{\partial E_z}{\partial t} = \frac{1}{\varepsilon_0 \varepsilon(x,y,z)}\left[\frac{\partial H_y}{\partial x} - \frac{\partial H_x}{\partial y}\right]. \quad (11)$$

If we consider the TE mode and solve for a plane, then the electrical permitivity can be expressed as $\varepsilon = \varepsilon(x,y)$. With this situation, the differential equations for TE mode are:

$$\frac{\partial H_x}{\partial t} = -\frac{1}{\mu_0}\frac{\partial E_z}{\partial y}, \quad (12)$$

$$\frac{\partial H_y}{\partial t} = \frac{1}{\mu_0}\frac{\partial E_z}{\partial x}, \quad (13)$$

$$\frac{\partial E_z}{\partial t} = \frac{1}{\varepsilon_0 \varepsilon(x,y)}\left[\frac{\partial H_y}{\partial x} - \frac{\partial H_x}{\partial y}\right]. \quad (14)$$

According to FDTD theory, these differential functions can be discretized in both space and time, so that they can be calculated as:

$$H_x^{n+1/2}(i,j+1/2) = H_x^{n-1/2}(i,j+1/2) - \frac{\Delta t}{\mu_0 \Delta y}\left\{E_z^n(i,j+1) - E_z^n(i,j)\right\}, \tag{15}$$

$$H_y^{n+1/2}(i+1/2,j) = H_y^{n-1/2}(i+1/2,j) - \frac{\Delta t}{\mu_0 \Delta x}\left\{E_z^n(i+1,j) - E_z^n(i,j)\right\}, \tag{16}$$

$$E_z^{n+1}(i,j) = E_z^n(i,j) + \frac{\Delta t}{\varepsilon_0 \varepsilon(i,j)}\left\{\begin{array}{l} \frac{1}{\Delta x}\left[H_y^{n+1/2}(i+1/2,j) - H_y^{n+1/2}(i-1/2,j)\right] - \\ -\frac{1}{\Delta y}\left[H_x^{n+1/2}(i,j+1/2) - H_x^{n+1/2}(i,j-1/2)\right] \end{array}\right\}. \tag{17}$$

In these equations Δx are Δy the spatial mesh steps along the coordinates *x* and *y* respectively, Δt is the time step, and the functions are discretized as follows: $F^n(i,j) = F(i\Delta x, j\Delta y, n\Delta t) = F(x,y,t)$.

We should solve the problem also for the TM mode. In this case the equations can be written as:

$$\frac{\partial E_x}{\partial t} = \frac{1}{\varepsilon_0 \varepsilon(x,y)}\frac{\partial H_z}{\partial y}, \tag{18}$$

$$\frac{\partial E_y}{\partial t} = -\frac{1}{\varepsilon_0 \varepsilon(x,y)}\frac{\partial H_z}{\partial x}, \tag{19}$$

$$\frac{\partial H_z}{\partial t} = -\frac{1}{\mu_0}\left[\frac{\partial E_y}{\partial x} - \frac{\partial E_x}{\partial y}\right]. \tag{20}$$

Again, discretizing these functions according to FDTD algorithm, we get:

$$E_x^{n+1}(i+1/2,j) = E_x^n(i+1/2,j) + \frac{\Delta t}{\varepsilon_0 \varepsilon(i,j)\,\Delta y}\frac{1}{\Delta y}\left\{H_z^{n+1/2}(i+1/2,j+1/2) - H_z^{n+1/2}(i+1/2,j-1/2)\right\}, \tag{21}$$

$$E_y^{n+1}(i,j+1/2) = E_y^n(i,j+1/2) - \frac{\Delta t}{\varepsilon_0 \varepsilon(i,j)\,\Delta x}\frac{1}{\Delta x}\left\{H_z^{n+1/2}(i+1/2,j+1/2) - H_z^{n+1/2}(i-1/2,j+1/2)\right\}, \tag{22}$$

$$H_z^{n+1/2}(i+1/2,j+1/2) = H_z^{n-1/2}(i+1/2,j+1/2) - \frac{\Delta t}{\mu_0}\left\{\begin{array}{l} \frac{1}{\Delta x}\left[E_y^n(i+1,j+1/2) - E_y^n(i,j+1/2)\right] - \\ -\frac{1}{\Delta y}\left[E_x^n(i+1/2,j+1) - E_x^n(i+1/2,j)\right] \end{array}\right\}. \tag{23}$$

As before, in these equations Δx are Δy the spatial mesh steps along the coordinates *x* and *y* respectively, Δt is the time step, and the functions are discretized as follows: $F^n(i,j) = F(i\Delta x, j\Delta y, n\Delta t) = F(x,y,t)$.

The implementation of the FDTD method was performed in a similar way to the diffusion method. The preferred results are those corresponding to the TE mode.

3. RESULTS AND DISCUSSION

3.1 Light diffusion equation

Numerical investigations of pulsed light propagation through highly scattering media have been performed for the wide range of typical optical parameters of biological samples. Let us consider in detail the case when a Gaussian-like light beam with the typical radius of $r_0 = 0.1cm$ and pulse duration $t_p = 20ps$ propagates in tissue. The tissue is characterized by absorption coefficient $\mu_a = 1cm^{-1}$, scattering coefficient $\mu_s = 50cm^{-1}$, anisotropy factor $g = 0.8$, and refractive

index $n = 1.35$. For these parameters the light beam interacts with tissue in quasi steady-state mode, since the typical diffusion time inside the medium $\tau_d = \frac{r_0^2}{Dv} \approx 20\,ps$, and it is comparable with pulse duration t_p.

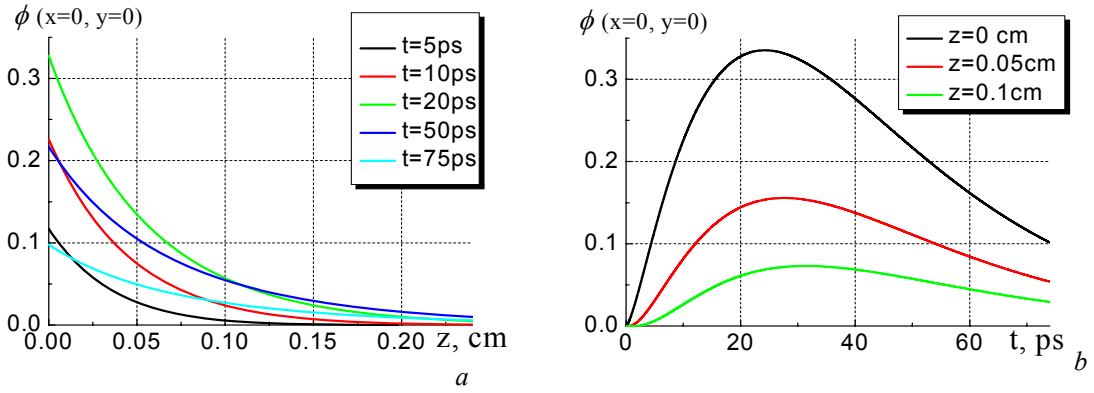

Fig. 1. Longitudinal distribution of irradiance in the cross-section of the light beam (*a*), and kinetics of irradiance at different depths inside the medium (*b*).

The results of simulation of this task are presented in Fig.1 and Fig.2. Figure 1a shows the on-axis distribution of the irradiance $\phi(x=0, y=0, z)$ in the tissue at different time moments. It is seen that the maximum of the irradiance is related to the pulse duration $t_p = 20\,ps$, and in the long-time limit the light is diffusively spreading inside the medium. Let us notice that efficient attenuation coefficient for this case is $\mu_{eff} = \sqrt{3\mu_a\left(\mu_a + \mu_s'\right)}$.

The kinetics of the irradiance at different depths inside the scattering medium is presented in Figure 1b for three reference points: $z = 0$, $z = 0.05cm$, and $z = 0.1cm$. The maximum value of the irradiance on the surface is formed with a little time shift regarding to t_p, and the formation of maxima of irradiance inside the medium depends on the depth along z-axis. Thus the diffusion wave is observed inside the scattering medium. And finally we consider the influence of scattering coefficient on spatial distribution of the irradiance inside the sample. Figure 2 shows radial distribution of irradiance in the cross-section of the light beam for $z = 0.05cm$ (a), and $z = 0.1cm$ (b). Increasing scattering coefficient leads to concentration of the light beam energy close to surface of the medium (Fig. 2a), and relative decreasing of the irradiance in the deeper cross-sections (Fig. 2b).

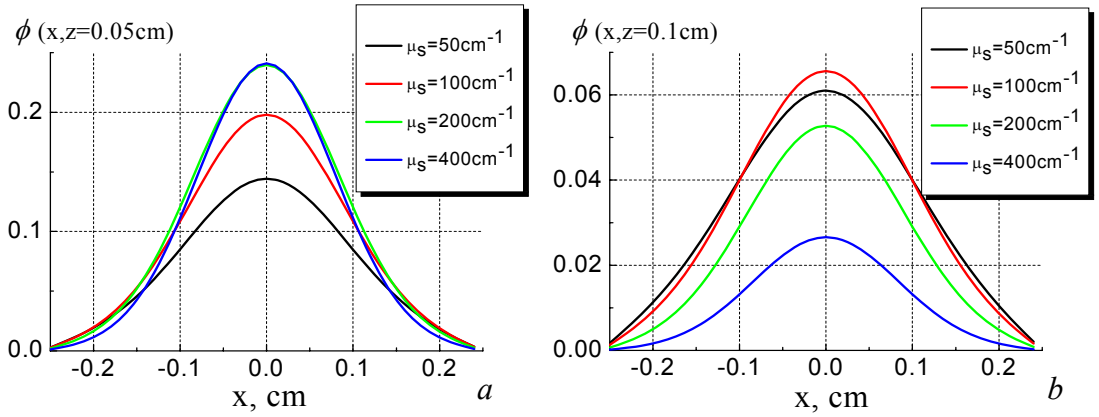

Fig. 2. Radial distribution of irradiance in the cross-section of the light beam. *a* – z=0.05cm, *b* – z=0.1cm.

3.2 FDTD numerical approach

A biological tissue model is needed in order to apply the FDTD approach. Optically turbid media are characterized by a strong scattering, which results in a scattering coefficient much higher than the absorption coefficient. The characteristics of the samples used in our simulations were chosen according to the typical characteristics of biological tissues [6]. From these data we have considered a mean spherical scattering particle diameter of 1μm, a volume fraction of scattering particles C=8%, a medium refractive index of n_0=1.34 (a volume average between extracellular fluid and cytoplasm) and a particle refractive index of n_0=1.45. The sample size was chosen to be 53.2μm by 53.2μm in order to obtain a representative sample, and as the same time maintaining a low calculation time. The square 2D sample matrix generated is shown in Figure 3a. In order to generate realistic 2D cuts of the spherical particles, we modeled the radius of the sphere cut as a stochastic process. The probability density function for the position of the cut point in the *z* axis of the sphere is simply given by a uniform distribution: $f(z) = 1/r_v$, $-r_v \le z \le r_v$, being 0 for the rest of values. In this equation, r_v denotes the radius of the spherical particle, and the reference point for z has been fixed in the center of the sphere. For a certain *z* position, if the cut intercepts a particle, the resulting circle diameter is simply given by: $r_s(z) = \left(r_v^2 - z^2\right)^{1/2}$.

From these equations, the average radius of the circles can be readily shown to be $\langle r_s(z) \rangle = \frac{\pi}{4} r_v$. Figure 3b shows the sample matrix generated according to the realistic modeling of turbid media sampling.

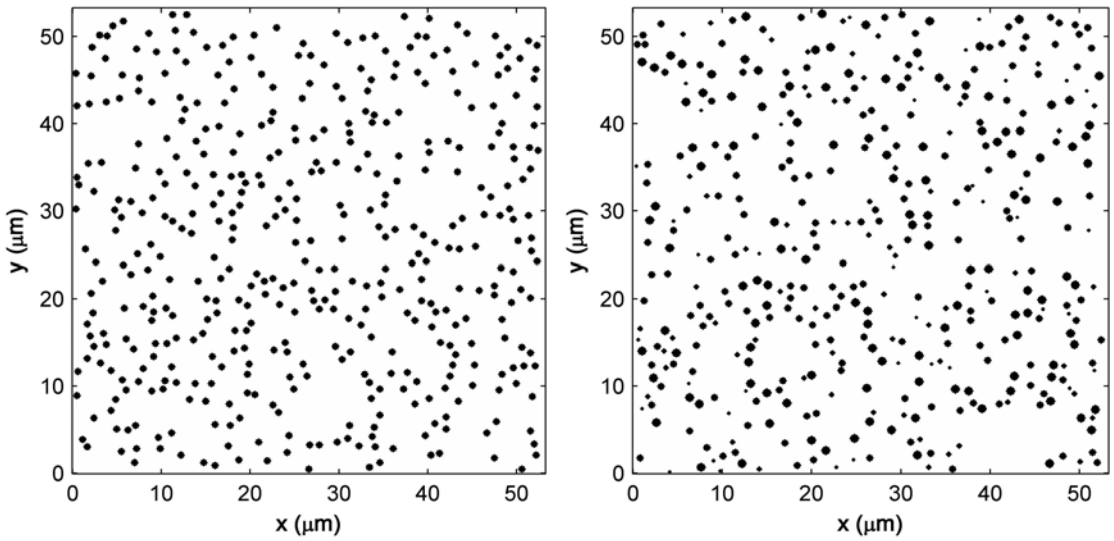

Fig. 3. Examples of scattering media. Number of particles N=433. a) – Spherical particle diameter *d*=1.00μm. b) – Mean cross-sectional particle diameter *d*=0.798 μm.

Using the theoretical model described in Section 2.2, light propagation thorough a turbid medium was analyzed. The FDTD results of the simulation of electro-magnetic waves propagation through this sample are shown in Figure 4, for a wavelength of $\lambda = 1.06\mu m$, corresponding to a Nd:YAG laser. Figure 4 presents the steady-state distribution of the optical power density for different concentration of scatterers. The influence of scattering can be clearly observed in the spatial distribution of optical power. In Figure 4b the spreading of optical radiation is much bigger than in Figure 4a, where the scatterers concentration is lower, and as a consequence the scattering events are not so often. Although the scattering is mainly forward-directed, it is evident how it affects the propagating beam, even for this small sample. If no scatterers were present, then there would be no spreading of the optical radiation as it travels through the biological sample.

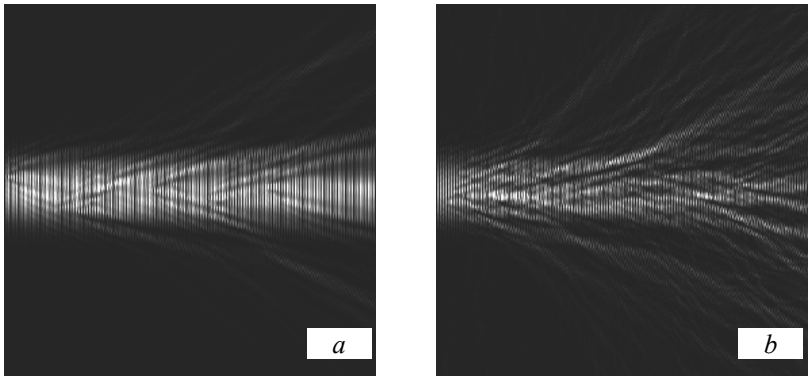

Fig. 4. Continuous light propagation through a turbid sample simulated with FDTD method. a – C=2%, b – C=8%.

After obtaining some previous results regarding continuous wave propagation, we substitute the continuous laser source by a pulsed source, and study the output pulse for different concentrations of scattering particles and for different sample thicknesses. Figure 5a shows the simulated results for a sample of thickness $L = 53.2\mu m$. It can be observed that the maximum pulse value decreases for larger particles concentrations. This result is in good agreement with the simple Beer-Lambert law. As well as that, we can also note that the pulse width increases with the scatterers concentration. These results are corroborated by those shown in Figure 5b, which corresponds to a tissue with twice the thickness, $L = 106.4\mu m$. Both effects, maximum pulse value decrease and pulse width increase with increasing number of scatterers, are larger in this second case. Note that the time scale varies in these two plots.

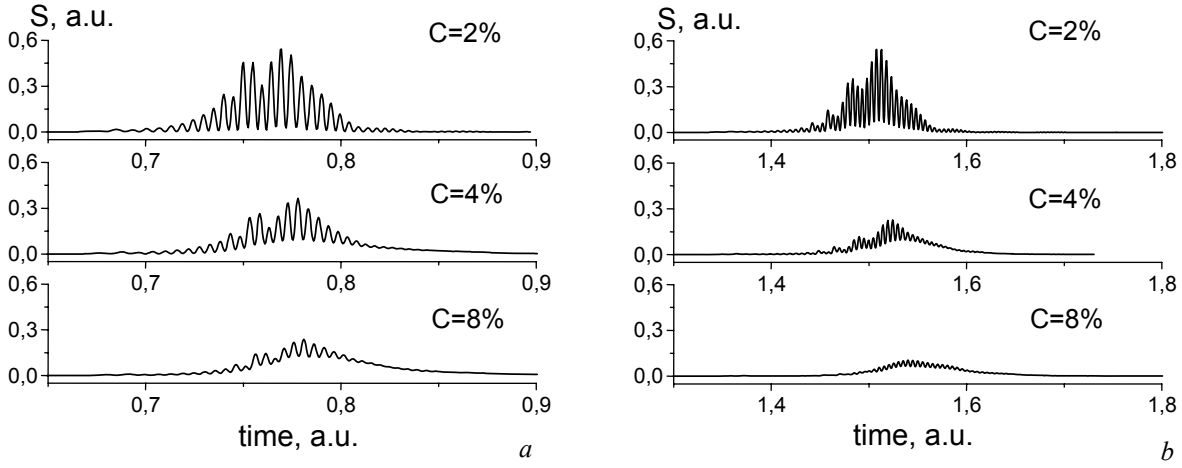

Fig. 5. Pulsed light propagation through a turbid medium. *a*) – Output pulses for a sample length of $L = 53.2\mu m$, *b*) – Output pulses for a sample length of $L = 106.4\mu m$.

4. CONCLUSIONS

In this work, optical propagation in biological tissues was analyzed by FDTD simulation. The results were focused on pulsed light propagation, as the analysis of continuous light propagation has been widely studied. FDTD light propagation approach was applied to several media with optical parameters in the typical range of those observed in biological tissues. The results show variations of pulsed light propagation as a function of the scatterers characteristics (namely size, concentration, and optical contrast). These variations were analyzed and discussed. The results were compared with those obtained by the diffusion approach, which does not carry all the information about the phase and coherence of the wavefront, but provide results in a smaller computational time.

The results of this work can be applied to a wide range of areas of interest like the time-resolved study of ultrashort light pulses propagation, the optimization of optical penetration depth, the coherence properties of pulsed light, and the effect of modified wavefronts in light propagation.

REFERENCES

[1] Boyd, R., [Nonlinear Optics], Academic Press, (1992).
[2] Vo-Dinh, T., [Biomedical Photonics Handbook], CRC Press, (2003).
[3] Wang, L., Jacques, S. L. and Zheng, L., "MCML – Monte Carlo modelling of light transport in multi-layered tissues", Computer Methods and Programs in Biomedicine 47, 131 (1995).
[4] Kawano, K. and Kitoh, T., [Introduction to Optical Waveguide Analysis: Solving Maxwell's Equations and the Schrodinger Equation], John Wiley and Sons, (2001).
[5] Fanjul-Vélez, F., Romanov, O. G. and Arce-Diego, J. L., "Efficient 3D numerical approach for temperature prediction in laser irradiated biological tissues", Computers in Biology and Medicine 39, 810 (2009).
[6] Romanov, O. G., Tolstik, A. L., Ortega-Quijano, N., Fanjul-Velez, F. and Arce-Diego, J. L., "Finite-Difference Time-Domain simulation of light propagation in 2D scattering media", Nonlinear Phenomena in Complex Systems 12, 267 (2009).
[7] Ortega-Quijano, N., Fanjul-Vélez, F., Salas-García, I., Romanov, O. G., Gorbach, D. V., Tolstik, A. L. and Arce-Diego, J. L., "Optical phase conjugation by dynamic holography for wavefront restoration in turbid media", Proc. SPIE 7562, 75620A (2010).
[8] E. C. Du Fort, S. P. Frankel, "Stability conditions in the numerical treatment of parabolic differential equations", Mathematical Tables and Other Aids to Computation 7, 135-152 (1953).
[9] V. K. Sauliev, [Integration of parabolic equations by the net methods], Fizmatgiz, Moscow, (1960).